

# Design procedure for the development of new floating floors to improve comfort on ships

Lorenzo Moro<sup>1)</sup>, Emanuele Brocco<sup>2)</sup>, Aglaia Badino<sup>3)</sup>, Pedro Nicolas Mendoza Vassallo<sup>2)</sup>,  
Alessandro Clericuzio<sup>3)</sup> and Marco Biot<sup>2)</sup>

<sup>1)</sup> Department of Ocean and Naval Architectural Engineering, Memorial University of Newfoundland, Canada

<sup>2)</sup> Department of Engineering and Architecture, University of Trieste, Italy

<sup>3)</sup> C.S.N.I. Scarl, Italy

## Abstract

*The paper presents a procedure developed for designing new floating floors for marine applications. The procedure aims at the improvement of the capability of a new floating floor to isolate structure borne noise. After an introduction to the theoretical background on which this procedure is built, the authors present the results obtained applying the developed procedure to a case study. The procedure includes numerical Finite Element simulations and experimental tests. The simulations aim at the optimization of the resilient material used to decouple the upper floor from the structures. The optimized configurations are then built and tested in laboratory. These tests allow the researchers to identify the floating floor resonances and to evaluate their effect on the Transmission Loss levels. The results of the research activity show the effectiveness of the developed procedure and highlight the importance of the experimental tests to validate the outcomes of the simulations.*

## Keywords

Structure borne noise isolation; floating floor; comfort; ships; transmission loss; dynamic experimental tests; experimental and numerical analysis.

## Introduction

Comfort on ships has become of paramount importance over the last few decades. As noise and vibration levels mostly affect the overall comfort level on ships, shipyards and research institutes have focused their research activity in the development of effective methods to control noise and vibration energy generated by on-board sources, and to mitigate noise and vibration levels on accommodation decks and on workplaces. These methods aim at different types of ships. Indeed, improving comfort on cruise ships and mega-yachts is a key factor to be competitive in the market. On the other hand, improving on-board comfort levels on other merchant vessels imply improving safety for crewmembers, as they are not exposed to hazardous noise and vibration levels in workplaces, and they can have proper rest in accommodation areas (DNV, 2009).

Several noise and vibration sources are installed on ships. Engines employed as prime movers or gen-sets, propellers, bow and stern thrusters, auxiliary machinery, HVAC systems and mooring systems are noise and vibration sources. Moreover, the entertainment system and human activities also increase noise and vibration levels on cruise vessels and mega-yachts. The acoustic energy generated by these sources is transmitted through the air (airborne noise) and through the structures (structure borne noise). In order to control the acoustic energy transmitted through the structures, the noise sources are usually resiliently mounted. This solution effectively isolates the sources only if the resilient mounting system is properly designed and then tested (Biot et al., 2014a, Biot et al., 2014b; Moro et al., 2013). The acoustic energy transmitted to the accommodation areas can also be controlled using floating floors and walls that isolate the receiver from the surrounding environment. In particular, floating floors are effective solutions to mitigate impact noise and structure borne noise (Kim et al., 2006; Cavanaugh et al., 2009). Therefore, a proper design of these devices should take into account both these aspects. Several research activities have been done in the recent years in order to characterize the impact acoustic isolation of floating floors for civil and marine applications. The outcomes of these researches provided insight into the influence of the dynamic stiffness of the resilient material on the Transmission Loss curve of the floating floor (Ramorino et al., 2003; Lin et al., 2005; Ladislav et al., 2007; Kulik et al., 2009; Schiavi et al., 2010), and on the development of high-performant materials (Faustino et al., 2012; Kino et al., 2012; Jahani et al., 2014; Nadal Gisbert et al., 2014). Moreover, other researchers focused their activity on the development of theoretical models for the prediction of the dynamic behavior of floating floors. Cha and Chun (2008) developed two theoretical models to predict the insertion loss of floating floors. The results achieved using these models were benchmarked against the outcomes of experimental tests. Cho (2013a; 2013b) investigated the influence of the frequency-matched resonances on impact sound transmission. The outcomes of numerical hybrid FE-SEA models were validated by the outcomes of experimental tests.

In the last decades, researchers have also focused their attention on the capability of floating floors to isolate the receiving room from stationary structure borne noise sources. The latter is an issue on civil buildings and dwellings, and on ships and marine structures. Oguç and Hadzikurtas (2015) investigated the capability of different floating floors to isolate the structure borne noise generated by machinery installed on concrete structures. Joo et al. (2009) performed a series of experimental tests that showed that noise level in ships' cabins is dominated by the acoustic energy transmitted by the cabin floor. Rizzuto (2000) and Ferrari and Rizzuto (2005) studied the damping effects of viscoelastic materials applied to ship structures. Viscoelastic materials are often applied to ship structures in order to dampen the vibration energy transmitted in the low frequency range as well as in the high frequency range (audio frequency range). Badino and Rizzuto (2015) investigated the isolation characteristics of a new material used as resilient element in a floating floor for marine application.

The state-of-the-art scientific literature review shows that even though several studies investigated the floating floors isolation performance, no design methods are available to control floating floors capability to mitigate structure borne noise levels, nor standard procedures to test their Transmission Loss.

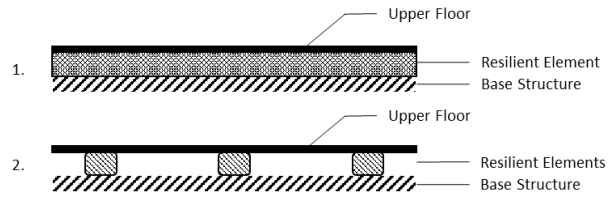
This paper presents the results of an on-going joint research activity among the University of Trieste, C.S.N.I., and Memorial University of Newfoundland. The aim of this project includes the development of a rational approach for the design of new floating floors taking into account their capability to mitigate structure borne noise level generated by steady sources. This procedure includes numerical simulations and experimental tests. The numerical simulations aim at the optimization of resilient mounting elements of floating floors in terms of dynamic stiffness and weight containment. The optimized configurations are then built and tested in laboratory. These tests allow the researchers to identify the floating floor resonances and to evaluate their effect on the Transmission Loss levels. The resilient mounting elements characterized by the highest levels of Transmission Loss levels will then be used to create floating floors that will be tested on a typical panel of ship deck.

Such a procedure is applied to develop a new floating floor that is considered as a case study. The results show the effectiveness of the developed procedure and pave the way for future developments of the research activity.

## Methods

Floating floors isolate an upper floor from a subfloor (i.e. ship structures) realizing a structural discontinuity. Floating floors for marine applications are usually divided into two groups: floating floors in which a continuous layer of decoupling material creates the discontinuity between the ship structures and the upper floor, and those ones in which resilient mounts are used as decoupling elements (Badino and Rizzuto, 2015). Fig. 1 shows the two different types of floating floors used on ships. The research activity presented in this paper deals with the design of

the resilient mounts employed in the second group of floating floors.



**Fig. 1: Two types of floating floor: 1. Floating floor with a continuous layer of decoupling material, 2. Floating floor with resilient mounts.**

## Theoretical background

Floating floors are usually tested in order to evaluate their performance in terms of impact sound insulation and airborne sound insulation. As far as structure borne noise isolation is concerned, no international standards exist. Nevertheless, some procedures have been developed by researchers in order to evaluate the capability of floating floors to reduce structure borne noise levels. (Ødegard, 2004)

A vibrating panel generates noise in the surrounding environment. The mechanical energy involved is often generated by remote sources that transmit audio-frequency vibrational energy through connected structures (Fahy, 2005). This is the case of ships, where engines and auxiliary machinery generate audio-frequency vibrational energy that is transmitted through the structures up to the accommodation decks (Moro et al, 2015). Sound pressure level generated in air at standard temperature by a panel excited by audio-frequency vibrational energy in the audio frequency range is obtained according to (Cremer et al, 2005):

$$L_p = L_v + 10 \log(A / 4S) - 10 \log \sigma \quad (1)$$

where  $L_p$  is the sound pressure level [dB ref 20  $\mu$ Pa],  $L_v$  is the velocity level [dB ref  $10^{-9}$  m/s] of the vibrating plate,  $A$  is the equivalent absorption area of the receiving room [ $m^2$ ],  $S$  is the radiating surface [ $m^2$ ] and  $\sigma$  is the radiation efficiency. The latter is obtained according to the following relation (Fahy, 2005):

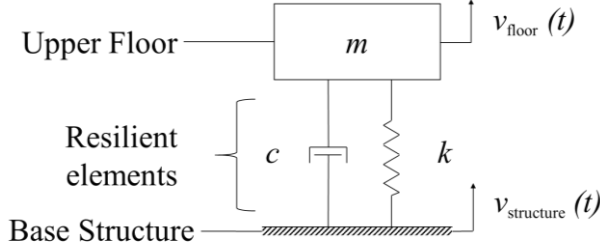
$$\sigma = \frac{W_{\text{radiated}}}{\rho c S \langle |v|^2 \rangle} \quad (2)$$

where  $W_{\text{radiated}}$  [W] is the sound power radiating from the vibrating surface,  $\rho$  is the air density [ $kg/m^3$ ],  $c$  is the sound velocity in air [m/s], and  $\langle |v|^2 \rangle$  is the effective value of the velocity of the radiator, averaged over the surface.

According to Eq. 1, if  $A$ ,  $S$  and  $\sigma$  are constant, which means that the acoustic characteristics of the receiving room and of the radiating panel are constant, the sound pressure level  $L_p$  generated by the vibrating panel decreases, decreasing the velocity level  $L_v$  of the vibrating panel.

As regards floating floors, the radiating surface is the upper floor, which radiates sound energy in the receiving room. If the dynamic characteristics of this surface are constant, the velocity level  $L_v$  of the upper floor can be

controlled improving the capability of the resilient element to reduce the transmitted vibrational energy. The floating floor can be considered as a damped single degree of freedom (SDOF) system suspended on a moving platform. Fig. 2 shows the scheme of the damped SDOF system, where  $m$  is the mass of the upper floor and of the resilient elements,  $k$  and  $c$  are respectively the equivalent stiffness and the damping coefficient of the resilient element.



**Fig. 2:** SDOF system that simulates, in a first approximation, a floating floor.

For this system we can define the mechanical mobility  $M_m$  of the mass system  $m$  as:

$$M_m = 1/mj\omega \quad (3)$$

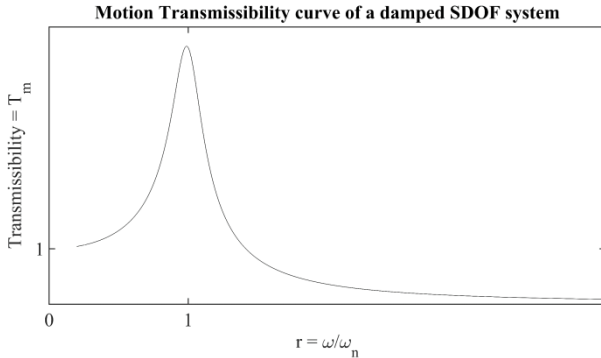
where  $j$  is the imaginary unit and  $\omega$  is the excitation frequency, and the mechanical mobility  $M_s$  of the damper  $c$  and spring  $k$  that are connected in parallel as:

$$M_s = 1/(c + (k/j\omega)) \quad (4)$$

The motion transmissibility  $T_m$  is defined as the ratio between the motion of the system  $v_{\text{floor}}$  and the applied support motion  $v_{\text{structure}}$ :

$$T_m = \left| \frac{v_{\text{floor}}}{v_{\text{structure}}} \right| = \left| \frac{M_m}{M_m + M_s} \right| \quad (5)$$

Fig. 3 shows a typical Transmissibility curve for a damped SDOF system. We can notice that in the very low frequency range the motion transmissibility tends to 1. As the exciting frequency increases and tends to the natural frequency of the system, the transmissibility curve increases up to its maximum value. Then, the transmissibility curve decreases and tends towards 0 as the frequency ratio tends to  $+\infty$ .



**Fig. 3:** Transmissibility curve of a damped SDOF system with support motion

The capability of a floating floor to isolate steady structure borne noise is often evaluated by researchers measuring its Transmission Loss (Ødegard 2004; Badino and

Rizzuto 2015). This is defined as:

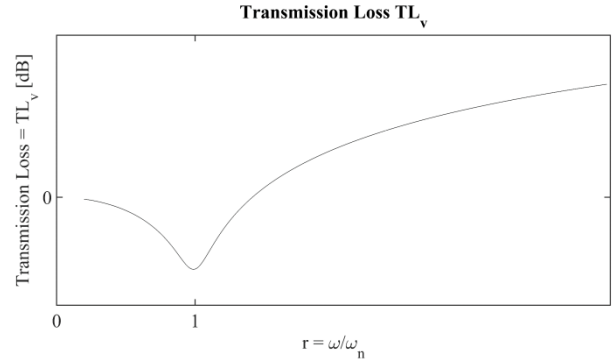
$$TL_v = L_{v,\text{structure}} - L_{v,\text{floor}} \quad (6)$$

where  $L_{v,\text{structure}}$  is the average velocity level of the deck structure [dB ref  $10^{-9}$  m/s], and  $L_{v,\text{floor}}$  is the average velocity level of the upper floor [dB ref  $10^{-9}$  m/s].

By combining Eq. 5 and Eq. 6 we obtain:

$$TL_v = 10 \log \frac{v_{\text{structure}}}{v_{\text{floor}}} = 10 \log \frac{1}{T_m} \quad (7)$$

Fig. 4 shows the Transmission Loss  $TL_v$  curve of a damped SDOF system. In this case, we can see that the Transmission Loss tends towards 0, as the frequency ratio  $r$  tends to 0. As the frequency ratio  $r$  increases towards 1, the Transmission Loss curve drops to a minimum. At higher frequency, the curve tends towards  $+\infty$  as the frequency ratio tends towards  $+\infty$ .



**Fig. 4:** Transmission Loss  $TL_v$  curve of a damped SDOF system

#### Procedure for the optimization of the resilient element of a floating floor

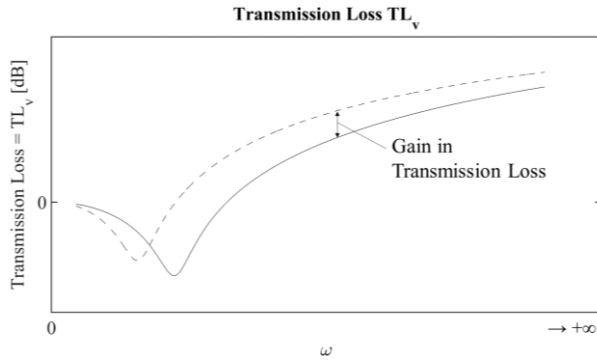
The authors developed a new procedure for the improvement of the isolation capabilities of floating floor resilient elements. According to Eq. 7, the Transmission Loss of a floating floor can be improved reducing the Transmissibility of its resilient elements. If the damping coefficient  $c$  of the resilient elements is constant, this can be achieved decreasing the equivalent stiffness  $k$  of the resilient mounting system. Fig. 5 shows the typical Transmission Loss curve of a floating floor (solid curve). Decreasing the equivalent stiffness  $k$  of the resilient elements, the natural frequency  $\omega_n = \sqrt{k/m}$  of the floating floor, considered as a damped SDOF system, decreases and so its resonant frequency decreases:

$$\omega_r = \omega_n \sqrt{1 - 2\zeta^2} \quad (8)$$

where  $\zeta$  is the damping ratio:  $\zeta = c/2\sqrt{km}$ .

This implies a shift of the Transmission Loss curve towards the left part of the graph (dashed curve in Fig. 5). The solid curve in Fig. 5 is the Transmission Loss of a damped SDOF system, and the dashed curve is the Transmission Loss of a damped SDOF system, that have the same inertia  $m$  and damping coefficient  $c$  of the previous SDOF system, but it is characterized by a lower value of stiffness  $k$ . Under the hypothesis that only the stiffness of the resilient element  $k$  decreases and that the mass  $m$  and the damping coefficient  $c$  are constant, the shift of the

Transmission Loss curve leads to an increase in the Transmission Loss curve in the high frequency range. With regards to the low frequency range, we can notice an increase of the Transmission Loss in correspondence of the resonant frequency. This is due to the fact that the maximum of the Transmissibility curve depends on the damping ratio  $\zeta$  (de Silva 2006). A decrease of the stiffness value  $k$  implies a decrease of the maximum of the Transmissibility curve and so, according to Eq. 7, an increase of the corresponding Transmission Loss curve. At frequencies lower than the resonant frequencies, the Transmission Loss decreases and tends to 0.



**Fig. 5:** Transmission Loss curves of two damped SDOF systems. The two systems have the same inertia  $m$  and the same damping  $c$ , but different stiffness  $k$ .  $k$  is lower in the system represented by the dash curve.

Even though decreasing the stiffness of the resilient elements implies an increasing of the Transmission Loss in the audio frequency range, it also implies higher deflection of the floating floor when it is subject to static loads. The static deflection of floating floor is considered as a constraint in the optimization process for the improvement of the dynamic response of the resilient elements.

The procedure for the optimization of the resilient elements of a floating floor developed in the research activity presented in this paper is structured as follows:

1. development of different configurations of the floating floor grillage modules,
2. development of finite element models of the floating floor grillage modules,
3. Static finite element analyses of the different configurations of the floating floor grillage modules subject to the design load,
4. experimental tests for measuring the static deflection of the prototypes of floating floor modules,
5. experimental tests for the dynamic characterization of the floating floor grillage modules.

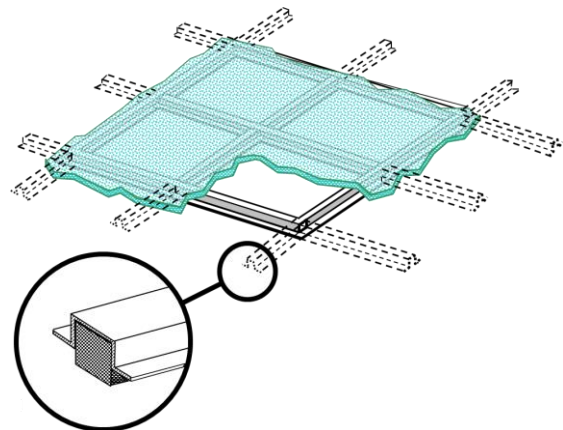
In the first phase of the procedure the researchers developed different configurations of the resilient elements, taking into account, beside the capability of the resilient element to isolate the floor, the feasibility of the resilient element, the ease of assemble and installation on board, and the overall cost for its production. Moreover, the overall weight of the floating floor was controlled over the development of the different configurations of the resilient elements.

Later, finite element models of the different configurations of the resilient elements were realized (Phase 2).

These models are used to evaluate the static deflection of the different configurations of the resilient mounts subject to the design static load. An iterative procedure is used in order to identify the lowest stiffness of the resilient element, and, at the same time, allows the floating floor to comply the design constraint of maximum deflection under a static compression load. The outcomes of the finite element analysis are a series of resilient elements that comply such design conditions (Phase 3). Then, Prototypes of these configurations of the resilient mount were built in laboratory and then tested (Phase 4). The first series of tests aims at the validation of the numerical simulations and allows the researchers to verify the stiffness of the prototypes of resilient mounts. Finally (Phase 5), the prototypes were tested in order to evaluate their dynamic characteristics in terms of resonant frequencies and Transmission Loss. The outcomes of these tests will include the Transmission Loss curve for each configuration of resilient elements. Comparing these curves the researchers are able to identify the resilient element that shows the highest performance in terms of Transmission Loss.

## Case Study

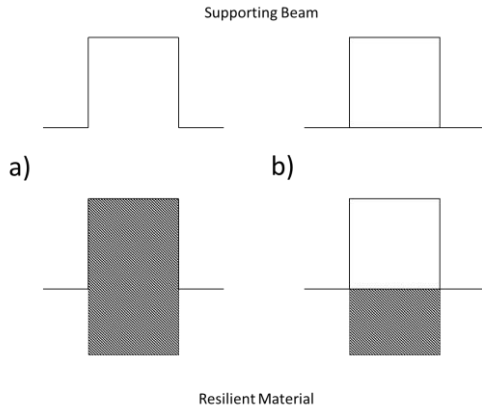
The procedure presented in the previous paragraph was implemented in order to optimize the performance of a new floating floor specifically designed to be installed on-board ships. This is a typical floating floor made of a grillage of hollow beams that are elastically suspended on a resilient element. The beams act as a support for both the noise isolation mineral wool panels, which are disconnected from the deck plating, and from the upper floor. Fig. 6 shows the floating floor grillage. The hollow beams are 0.6 m long, and, in its original configuration, 2 mm thick. The material employed as resilient element is continuously distributed beneath the hollow beams.



**Fig. 6:** Floating floor grillage considered as a case study. The typical transverse section of the hollow beam is shown.

In the first phase, several configurations of the floating floor resilient element were developed. The aim was to improve the dynamic characteristics of the resilient element in order to maximize the floating floor Transmission Loss. Two different transverse sections of the hollow beam were taken into account: closed section and open section (Fig. 7). These two different configurations

were built using two thicknesses: 1 mm and 2 mm.



**Fig. 7:** transverse section of the hollow beam and of the resilient element in the two different configurations: a) open, b) closed

Two different materials were used to create the decoupling element: viscoelastic material and rubber. Moreover, the resilient material was also considered in two different configurations: continuous and discontinuous. The geometric layout of the grillage was considered constant as it was harmonized with the stiffening spacing of a typical deck structure. Once the different configurations were identified, finite element (FE) models were developed for each configuration. Each FE model represents just one module of the grillage. Later, a series of FE linear static analysis was performed in order to evaluate the static deflection of the resilient element subject to the design static load. The latter was chosen according to the experience of the researchers as a vertical distributed compression load  $P_{\text{floor}}$  equals to  $2450 \text{ N/m}^2$ . Each FE model was loaded with this static load and iterative simulations were performed in order to evaluate the static deflection of the resilient element, varying the stiffness (i.e. the Young Modulus  $E$  of the resilient element). The maximum allowable static deflection  $d_{\text{max}}$  was set equal to 1 mm. This value was chosen in consideration of the fact that a higher deflection of the floating floor could lead to a feeling of discomfort for passengers and crew members while walking on the floor.

The outcomes of these simulations allowed the researchers to identify six different configurations to test in laboratory. The prototypes of these configurations were built and tested. In particular, a first series of test were performed in order to evaluate the static deflection of the prototypes and to validate the numerical FE models. The resilient elements were loaded with the design load  $P_{\text{floor}}$  and the static deflection were measured. Later, dynamic tests were performed in order to evaluate the resonant frequency of the damped SDOF system made by the resilient element and a mass that was placed on the resilient element in order to simulate the upper floor mass. The outcomes of these tests also allowed the researchers to identify the dynamic stiffness of the resilient elements for each configuration.

After this series of tests, another series of test was carried out for the measurement of the Transmission Loss of the resilient elements of the floating floors.

### Identification of the different configurations

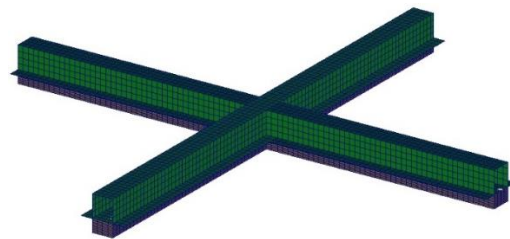
The configuration a) showed in Fig. 7 was considered as the basic configuration in the optimization process. Building on the theoretical considerations previously presented, the researchers identified different configuration of the floating floor grillage module. These configurations differ from each other for the shape of the beam section, for its thickness, for the resilient material and for its application beneath the supporting beam. Indeed, the material was applied continuously or discontinuously. The latter configuration was take into account by the researchers in order to minimize the weight of the optimized floating floor. Table 1 shows the different configurations that were taken into account in the optimization process.

**Table 1:** Different configurations of the floating floor grillage module taken into account in the optimization process.

Config.	Beam	Thick. [mm]	Application	Material
0		2	Cont.	Visco.
1		1	Cont.	Visco.
2		2	Cont.	Visco.
3		1	Cont.	Visco.
4		2	Discont.	Visco.
5		1	Discont.	Visco.
6		2	Cont.	Rubber
7		1	Cont.	Rubber
8		2	Discont.	Rubber
9		1	Discont.	Rubber

### Finite Element analysis of the resilient elements

Finite element models were created in order to evaluate the stiffness of the resilient material to be used in the floating floor. As the resilient element system of the floating floor is made of modules (Fig. 6), one single module was modelled. Fig. 8 shows the FE model of a module of the grillage. This module corresponds to the configuration 4 (Table 1).



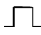
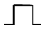
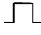
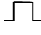
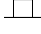
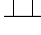

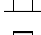
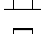

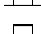
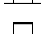
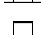


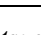
**Fig. 8:** Finite element model of a module of the floating floor.

The beam was modelled with low order quadrilateral shell elements (2D) with four nodes, while the resilient material was modelled with fully integrated linear brick elements (3D) with eight nodes. The model was loaded with the design static compression load ( $P_{\text{floor}}=2450 \text{ N/m}^2$ ) applied to the top surface of the module. The material of the resilient element and of the beam were simulated as an elastic material. This assumption is valid as

the resilient element is supposed to work under small deformation and so its stiffness does not change during loading.

The aim of the simulations was to identify the lowest stiffness of the resilient material in order to improve the Transmission Loss curve of the resilient element. At the same time, the resilient material stiffness should allow the floating floor to comply with the design limit of maximum displacement  $d_{\max}$  under compression load. The latter was selected equal to 1 mm. In the simulations of the modules with viscoelastic material used as resilient material, two different Young modulus  $E$  were considered: 0.73 MN/m<sup>2</sup>, and 0.472 MN/m<sup>2</sup>. These values resulted from a first analytical analysis of the minimum allowable stiffness of the resilient element subject to the design load. Moreover, these values of the Young modulus take into account the technological limitations in the control of the stiffness of the viscoelastic material, during its production. With regards to the rubber material, as it was selected among products available in the market, its Young modulus  $E$  was selected equal to 4.4 MN/m<sup>2</sup>. In Table 2, the bold types highlight the configurations that do not comply with the design constraint of maximum deflection  $d_{\max} \leq 1$  mm. In the Table,  $f_n$  are the natural frequencies.

**Table 2: Results of the linear static finite element analysis of the different configurations of the floating floor grillage modules.**

Config.	Beam	$E$ [MN/m <sup>2</sup> ]	Displ. [mm]	$f_n$ [Hz]
0A		0.725	0.930	15.7
<b>0B</b>		<b>0.472</b>	<b>1.430</b>	<b>12.6</b>
1A		0.725	0.946	15.5
<b>1B</b>		<b>0.475</b>	<b>1.446</b>	<b>12.6</b>
2A		0.725	0.642	18.9
2B		0.475	0.986	15.2
3A		0.725	0.666	18.5
<b>3B</b>		<b>0.475</b>	<b>1.010</b>	<b>15.0</b>
4A		0.725	0.963	15.4
<b>4B</b>		<b>0.475</b>	<b>1.479</b>	<b>12.4</b>
<b>5A</b>		<b>0.725</b>	<b>1.516</b>	<b>12.3</b>
<b>5B</b>		<b>0.725</b>	<b>1.002</b>	<b>15.1</b>
6		4.4	0.184	35.2
7		4.4	0.162	37.5
8		4.4	0.274	28.9
9		4.4	0.244	30.6

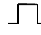
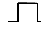




**Laboratory tests: static deflection of the floating floor under static compression load**

The results of the FE simulations allowed the researchers to identify the minimum allowable stiffness of the resilient material of the floating floor. This implies that the researchers were able to identify a minimum Young Modulus  $E$  of the resilient material. Building on the outcomes of the numerical analysis, six prototypes of a module of floating floor grillage were designed and built to be tested in laboratory. In this phase of the research activity, only the configurations with beam thickness of 2 mm were

tested. The configurations tested in laboratory (Table 3) include the basic configuration, characterized by open section of the module beam and high stiffness of the viscoelastic material, which is continuously distributed inside the beam (Conf. A).

The first series of laboratory tests aimed to check the compliance of the prototypes with the design specifications on the maximum allowable static deflection  $d_{\max}$  under a static compression load. A distributed load of 2450 N/m<sup>2</sup> was applied to each prototype. The measurement of the static deflection was undertaken after 24h, in order to allow the relaxation of the resilient material (Moro et al., 2015). Each measurement was undertaken using an indicator. The last column of Table 3 shows the results in terms of displacement. According to these results, only the configuration 8 did not comply with the maximum displacement limit  $d_{\max}=1$  mm. It is worth pointing out that there is a large discrepancy between the outcomes of the numerical simulations and those obtained by the experimental tests. These discrepancies are due to the difficulty in controlling the stiffness of the viscoelastic material during its manufacturing process. This can also explain the discrepancy showed by the numerical simulation of the modules with the rubber material and the correspondent experimental results.

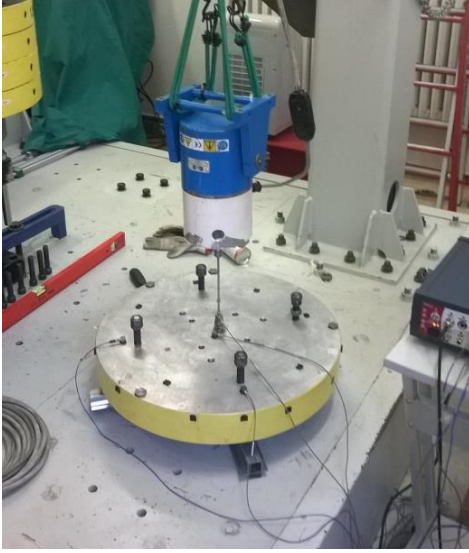
**Table 3: Results of the laboratory tests for the measurement of the static deflection of the floating floor grillage module subject to the design static load**

Config.	Beam	Application	Displ. [mm]
0		Continuous	0.37
0A		Continuous	0.64
2A		Continuous	0.50
4A		Discontinuous	0.80
6		Continuous	0.63
<b>8</b>		<b>Discontinuous</b>	<b>1.48</b>

**Laboratory tests: dynamic characterization of the floating floor modules**

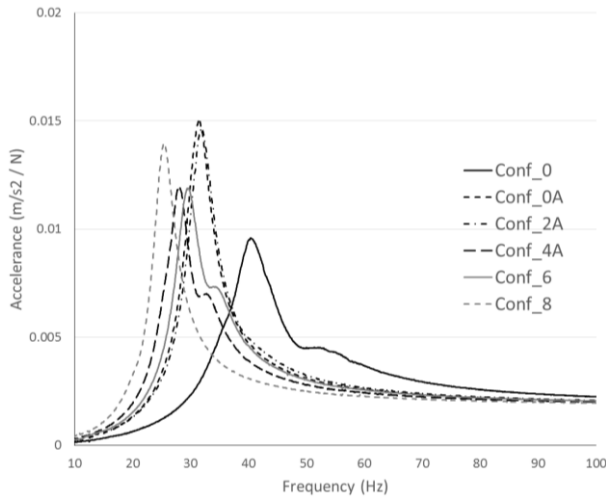
After the experimental static tests, a series of dynamic experimental tests was performed on the same configurations tested in the static tests (Table 3). These aimed at the measurement of the damped natural frequency of the damped SDOF system made of the floating floor grillage module prototypes and a mass that was selected to simulate the upper floor.

Fig. 9 shows the experimental apparatus employed to measure the resonant frequency of the system. The resilient element lays on a rigid plane surface and supports the mass used to simulate the upper surface. The two parts are fastened together using bolted joints. An electrodynamic shaker is used to excite the system. It is connected to the upper mass by a stinger rod. A 12 channel data acquisition system was used to acquire the data measured by ICP piezoelectric accelerometers and by an ICP dynamic load cell that was connected to the stinger rod and to the upper mass. The data acquisition system was also used to condition the acquired analog signal and to convert it to a digital signal.



**Fig. 9:** Experimental apparatus used for the measurement of the damped natural frequencies of the modules

A laptop was used to analyze the signal in frequency domain and to calculate the frequency response functions (FRF) obtained as ratio between the acceleration measured by each accelerometer and the force signal (Acceleration [m/s<sup>2</sup>N]). The FRF were calculated in terms of H1 and H2 estimators in order to evaluate the effect of unwanted input vibrations on the measured data (de Silva 2006). Moreover, the coherence functions were calculated in order to verify the quality of the measured data. As the calculated natural frequencies ranged between 12 Hz and 36 Hz, a white noise signal has been used to excite the system. This ranged between 1 Hz and 100 Hz.



**Fig. 10:** Accelerance functions in the vertical direction of the floating floor modules.

The tests were carried out for each prototype of the floating floor grillage module (Table 3). Fig. 10 shows the results of the experimental tests in terms of Accelerance functions.

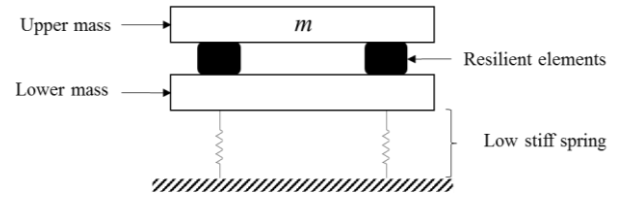
As shown in the graph, the decreasing of the resilient material stiffness implies a decrease of the damped natural frequency of the system, considered as a damped SDOF system. Table 4 shows the damped natural frequencies measured in the experimental tests. In the Table,  $f_r$  is the resonant frequency expressed in Hz.

**Table 4:** Modules damped natural frequencies measured in the experimental tests

Config.	Beam	$f_r$ [Hz]
0		37.5
0A		29.5
2A		37.5
4A		26.5
6		29.5
8		27.0

Later, a series of tests were carried out in order to measure the Transmission Loss of each floating floor grillage module. Fig. 11 shows the schema of the experimental apparatus used in the experimental tests. The upper mass is bolted to the resilient element which lays on a lower mass. The latter is decoupled from a rigid base by means of soft springs.

The stiffness of these springs was selected considering that the natural frequency of the SDOF system composed by the lower mass and the soft springs  $\omega_{nl}$  should be  $\omega_{nl} \leq 1/3 \omega_n$ , where  $\omega_n$  is the natural frequency of the resilient module and the upper mass, considered as a SDOF system. This guarantees that the system can be considered decoupled from the rigid base (Moro et al. 2013).



**Fig. 11:** Schema of the experimental layout for the measurement of the damped natural frequencies of the modules

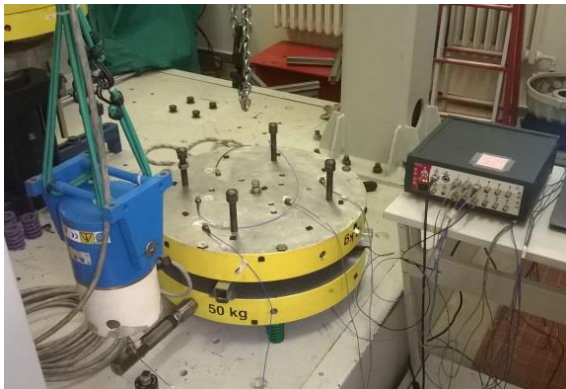
The electrodynamic shaker was connected to the lower mass by means of a stinger rod. ICP piezoelectric accelerometers were attached to the upper surface of the upper mass as well as to the lower surface of the lower mass (Fig. 12). A 12 channel data acquisition system was used to acquire the data, condition the signals and supply the sensors. The input signal was white noise which ranged between 5 Hz and 5 kHz. In the tests, each module was loaded with the upper mass and the dynamic tests were carried out after 24 hours, in order to allow the relaxation of the resilient material.

The acceleration levels acquired by each accelerometer on the upper surface of the upper mass were than averaged in order to evaluate the velocity level on the upper surface, according to the following formula:

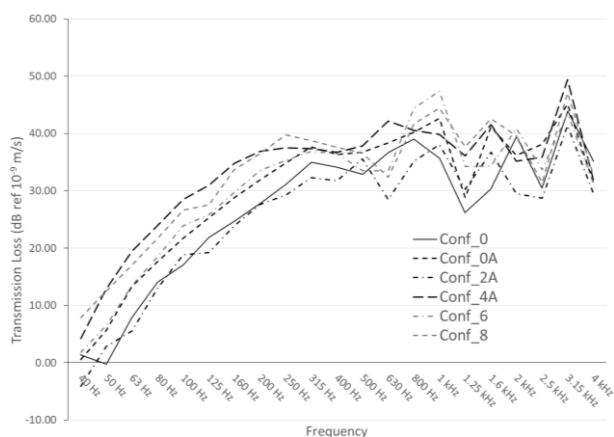
$$L_{v, \text{floor}} = 10 \log \left( \frac{1}{10} \sum_{i=1}^n 10^{\frac{L_{v,i}}{10}} \right) \quad (9)$$

where  $L_{v,i}$  is the velocity level [dB ref 10<sup>-9</sup> m/s] measured at the  $i$ -point of the upper surface of the upper mass. The same formula was used to calculate the average velocity levels  $L_{v, \text{structure}}$  of the lower surface of the lower mass.

The resulting average velocity levels are showed in Fig. 13.



**Fig. 12: Experimental apparatus used for the measurement of the damped natural frequencies of the modules**



**Fig. 13: Transmission Loss curves of the floating floor grillage modules**

According to the theoretical considerations presented before, in the neighborhood of their damped natural frequencies all the Transmission Loss curves tend to zero ( $f \leq 40$  Hz). As the frequency increases, the curves increase about linearly in the log-log graph. Moreover, we can see a general trend of the Transmission Loss curves which increase their values as the stiffness of the resilient material decreases. In particular, the stiffest modules (Conf 0 and Conf 2A) are characterized by the lowest Transmission Loss. On the other hand, the Conf. 4A and Conf 8, which are characterized by the lowest stiffness of the resilient materials, are characterized by the highest value of Transmission Loss. Afterwards, the curves deviate from their ideal behavior and a series of peaks are shown. This means that the modules no more behave as a damped SDOF system. Indeed, at high frequencies, the floating floor module beams no more behave as rigid bodies and this affect the overall behavior of the module. Moreover, the same consideration can be made as regards the upper floor. In this case, an aluminum disk was considered to simulate the upper floor. The outcomes of dynamic simulations performed to evaluate its dynamic behavior showed that its first mode appears at 1.25 kHz. This is reflected by the drop of the Transmission Loss curves in this 1/3 octave band.

## Conclusion

The paper presents the results of an optimization process

which aims at the improvement of the capability of a floating floor for marine application to isolate on-board structure borne noise. After an introduction to the theoretical background on which the procedure is built, the authors present the results of numerical and experimental tests carried out to improve the isolation effect of a floating floor. The results of the experimental activities show the effectiveness of the developed procedures. In particular, the outcomes of the measurements undertaken to evaluate the Transmission Loss curves show that the floating floor can be considered as a SDOF system in the low frequency range. In the high frequency range, the Transmission Loss curves deviate from the ideal behavior as the dynamics of the floating floor components affect the overall Transmission Loss. Nevertheless, the authors highlighted the discrepancy showed when the outcomes of the numerical simulations are benchmarked against the results of the experimental tests. This is due to the manufacturing process for the fabrication of the resilient material. Indeed, during this process the physical characteristics of this material are difficult to control. This does not affect the significance of the numerical simulations that provides the researchers with useful information on the stiffness limits of the resilient materials, but it implies that the experimental tests presented in this paper should always be carried out in order to verify the actual characteristics of the material. The research activity is carrying on and the experimental tests presented in this paper will be performed on the configurations with the hollow beam thickness equal to 1 mm. Finally, the selected modules will be used to build floating floors that will be tested in order to verify the effectiveness of the optimized solutions when applied to full-scale floating floors.

## References

- Badino, A, and Rizzuto, E (2015) "Innovative de-coupling materials for the isolation of ship cabins", Maritime Technology and Engineering, Taylor and Francis Group, pp 565-573.
- Biot, M, Boote, D, Brocco, E, Mendoza Vassallo, PN, Moro, L, and Pais, T (2014a). "Validation of a design method for the simulation of the mechanical mobility of marine diesel engine seating", 18th International Conference on Transport Means, RANSPORT MEANS 2014, Kaunas, pp 376-379
- Biot, M, Moro, L, and Mendoza Vassallo, PN (2014b). "Prediction of the structure borne noise due to marine diesel engines on board cruise ships", Proc 21st International Congress on Sound and Vibration 2014, ICSV 2014, Vol 3, pp 2513-2520.
- Cavanaugh, WJ, Tocci, GC, and Wilkes, JA (2009). "Architectural Acoustics: Principles and Practice", 2nd Edition, Wiley & Sons, Inc.
- Cha, SI, and Chun, HH (2008). "Insertion loss prediction of floating floors used in ship cabins", Applied Acoustics, Vol 69, No 10, pp 913-917.
- Cho, T (2013a). "Vibro-acoustic characteristics of floating floor system: The influence of frequency-matched resonance on low frequency impact sound", Journal of Sound and Vibration, Vol 332, No 1, pp



- Cho, T (2013b). "Experimental and numerical analysis of floating floor resonance and its effect on impact sound transmission", *Journal of Sound and Vibration*, Vol 332, No 25, pp 6552-6561.
- Cremer, L, Heckl, M, Pertersson, BAT (2005). "Structure borne Sound: Structural Vibrations and Sound Radiation at Audio Frequencies", Springer Berlin Heidelberg, Berlin.
- De Silva, CW (2006). "Vibration: fundamentals and practice", CRC Taylor & Francis, New York
- DNV (Det Norske Veritas) (2009). "Quieter offshore vessels are safer ships", *Motor Ships*, Vol 90, pp 28-30.
- Fahy, F (2005). "Foundation of engineering acoustics", Elsevier Academic Press, San Diego CA.
- Faustino, J, Pereira, L, Soares, S, Cruz, D, Paiva, A, Varum, H, Ferreira, J, and Pinto, J (2012). "Impact sound insulation technique using corn cob particleboard", *Construction and Building Materials*, Vol 37, pp 153-159.
- Ferrari A, and Rizzuto, E (2005). "Modal behaviour of a full-scale deck panel with anti-noise treatments", *Proc. 12th Congress of International Maritime Association of the Mediterranean, IMAM 2005*, Vol 1, pp 395-403.
- Jahani, D, Ameli, A, Jung, PU, Barzegari MR, Park, CB, and Naguib, H (2014) "Open-cell cavity-integrated injection-molded acoustic polypropylene foams", *Materials and Design*, Vol 53, pp 20-28.
- Joo, WH, Kim, SH, Bae, JG, and Hong, SY (2009). "Control of radiated noise from a ship's cabin floor using a floating floor", *Noise Control Engineering Journal*, Vol 57, No 5, pp 507-514.
- Kim, HS, Kim, BK, Cha, SI, and Kim, YS (2006). "Floor impact noise reduction in ship cabins by means of a floating floor", *Noise Control Engineering Journal*, Vol 54, No 6, pp 406-413.
- Kino, N, Nakano, G, and Yasuhiro, S (2012) "Non-acoustical and acoustical properties of reticulated and partially reticulated polyurethane foams", *Applied Acoustics*, Vol 73, No 2 pp 95-108.
- Kulik, VM, Semenov, BN, Boiko, AV, Seoudi, BM, Chun, HH, and Lee, I (2009). "Measurement of dynamic properties of viscoelastic materials", *Experimental Mechanics*, Vol 49, pp 417-425, 2009.
- Ladislav, P, Ludek, P, Frantisek, V, and Jan, C (2007). "Laboratory measurement of stiffness and damping of rubber element". *Engineering Mechanics*, Vol. 14, No 1/2, pp 13-22.
- Lin, TR, Nabil, H, Farag, I, and Pan, J (2005). "Evaluation of frequency dependent rubber mount stiffness and damping by impact test". *Applied Acoustics*, Vol 66, pp. 829-844.
- Oguc, M, and Hadzikurtes, D (2015) "Acoustic Evaluation of Floating floor applications in mechanical rooms", *Proc 10th European Congress and Exposition on Noise Control Engineering, EuroNoise 2015, Maastricht* pp 2521-2524.
- Moro, L, Biot, M, Mantini, N, and Pestelli, C (2013). "Solutions to improve accuracy in experimental measurement of the dynamic response of resilient mountings for marine diesel engines". *Proc 4th International Conference on Marine Structures, MARSTRUCT 2013, Espoo*, pp 355-363.
- Moro, L, Brocco, E, Mendoza Vassallo, PN, Le Sourne, H and Biot, M (2015). "Numerical simulation of the dynamic behaviour of resilient mounts for marine diesel engines", *Proc. 5th International Conference on Marine Structures, MARSTRUCT 2015*, pp. 149-157
- Nadal Gisbert, A, Gadea Borrell, JM, Parres García, F, Juliá Sanchis, E, Crespo Amorós, JE, Segura Alcaraz, J, and Salas Vicente, F (2014). "Analysis behaviour of static and dynamic properties of Ethylene-Propylene-Diene-Methylene crumb rubber mortar", *Construction and Building Materials*, Vol 50, pp 671-682.
- Ødegard, I (2004). "Sound Insulation Properties of Marine Flooring Constructions Manufactured by Sika Cufaden A/S. Technical Report. Fredensborg.
- Ramorino, G, Vetturi, D, Cambiaghi, D, Pegoretti, A, and Ricco, T (2003). "Development in dynamic testing of rubber compounds: assessment of non-linear effects", *Polymer Testing*, Vol 2, pp 681-687.
- Rizzuto, E (2000). "Viscoelastic Materials for noise reduction on board" *Proc 9th Congress of International Maritime Association of Mediterranean, IMAM 2000*, Vol 3, pp 61-68.
- Schiavi, A, Pavoni Belli, A, and Corallo, M (2010). "Dynamic stiffness of resilient materials: some consideration on the proposed revision of ISO 9052-1 standard", *Proc. 20th International Congress on Acoustics, ICA 2010*.